Journal of Chromatography A, 1218 (2011) 2528–2539

Contents lists available at ScienceDirect

Journal of Chromatography A

journal homepage: www.elsevier.com/locate/chroma

Isolation of phosphopeptides using zirconium-chlorophosphonazo chelate-modified silica nanoparticles

Pei-Xuan Zhao[a], Yong Zhao[b], Xiao-Feng Guo[a], Hong Wang[a,*], Hua-Shan Zhang[a]

[a] Key Laboratory of Analytical Chemistry for Biology and Medicine (Ministry of Education), Department of Chemistry, Wuhan University, Wuhan 430072, China
[b] College of Life Sciences, Wuhan University, Wuhan 430072, China

ARTICLE INFO

Article history:
Received 21 January 2011
Received in revised form 28 February 2011
Accepted 28 February 2011
Available online 4 March 2011

Keywords:
Zirconium-chlorophosphonazo
chelate-modified silica nanoparticles
Phosphopeptide enrichment
Human serum
MALDI-TOF MS

ABSTRACT

Due to the low abundance of phosphoproteins and substoichiometry of phosphorylation, the elucidation of protein phosphorylation requires highly specific materials for isolation of phosphopeptides from biological samples prior to mass spectrometric analysis. In this study, chlorophosphonazo type derivatives of chromotropic acid including *p*-hydroxychlorophosphonazo (HCPA) and chlorophosphonazo I (CPA I), traditionally used in the photometric determination of transition metal ions, have been employed as chelating ligands in the preparation of novel affinity materials for phosphopeptide enrichment. The chromogenic reagents of HCPA and CPA I were chemically modified on the surface of silica nanoparticles, and the functionalized materials were charged with zirconium ions through the strong complexation between chelating ligands and Zr^{4+}. The obtained zirconium-chlorophosphonazo chelate-modified silica nanoparticles (Zr-HCPA-SNPs and Zr-CPA I-SNPs) were applied to the selective enrichment of phosphopeptides, followed by matrix-assisted laser desorption/ionization time-of-flight mass spectrometry (MALDI-TOF MS) analysis. The purification procedures were optimized using α-casein digest at first, and then the performance of these two affinity materials for efficient and specific enrichment of phosphopeptides was evaluated with the tryptic digests of standard proteins (α-casein, β-casein, ovalbumin and bovine serum albumin). It is found that Zr-HCPA-SNPs are superior to Zr-CPA I-SNPs in phosphopeptide enrichment. Using Zr-HCPA-SNPs to trap phosphopeptides in α-casein digest, the detection limit was close to 50 fmol based on MALDI-TOF MS analysis. Finally, Zr-HCPA-SNPs were used to directly isolate phosphopeptides from diluted human serum of healthy, diabetes and hypertension persons, respectively. Our results show that the constitution and level of phosphopeptides are remarkably different among the three groups, which indicate the powerful potentials of Zr-HCPA-SNPs in disease diagnosis and biomarker screening.

1. Introduction

Reversible phosphorylation of proteins is one of the most ubiquitous post-translational modifications (PTMs) in nature, which plays a vital role in regulating many important biological processes and functions such as cell proliferation, differentiation, signal transduction and metabolic maintenance [1–3]. It has been estimated that approximately one-third of the proteins *in vivo* in a given mammalian cell are phosphorylated at any time point [4]. Therefore, to isolate phosphopeptides and ascertain the phosphorylation sites are of great importance in proteome research. Analytical techniques applied for analysis of phosphorylation sites include ^{32}P labeling, Edman sequencing, mass spectrometry (MS), etc. [5–7]. MS-based methods, such as matrix-assisted laser desorption/ionization mass spectrometry (MALDI MS) [8–10] and electrospray ionization mass spectrometry (ESI MS) [11,12], are powerful tools for protein phosphorylation analysis. However, large-scale analysis of protein phosphorylation sites by MS is still a big challenge because of the low abundance of phosphoproteins in tissues or cells, poor ionization efficiency of phosphopeptides and signal suppression by nonphosphopeptides in mass spectra [5,6]. Thus, enrichment methods that reduce sample complexity and increase the relative concentration of phosphoproteins or phosphopeptides have been in demand before MS analysis.

Enrichment approaches for this purpose have been developed rapidly, such as immunoprecipitation [13,14], chemical reactions through β-elimination/concurrent Michael addition [15,16], immobilized metal ion affinity chromatography (IMAC) [17–20], metal oxide affinity chromatography (MOAC) [21,22], and strong cation/anion exchange chromatography (SCX/SAX) [23,24]. IMAC is widely used to enrich phosphopeptides. However, conven-

* Corresponding author. Tel.: +86 27 87218924; fax: +86 27 68754067.
E-mail address: hongwang@whu.edu.cn (H. Wang).

0021-9673/$ – see front matter © 2011 Elsevier B.V. All rights reserved.
doi:10.1016/j.chroma.2011.02.071

tional affinity materials usually adopt iminodiacetic acid (IDA) and nitrilotriacetic acid (NTA) as chelating ligands for immobilization of metal ions, which lack enough selectivity of phosphoproteome analysis. Accordingly, it is still crucial to exploit novel affinity materials (chelating ligands, immobilized metal ions, supports, etc.) to achieve specific and efficient enrichment of phosphopeptides.

The chlorophosphonazo type derivatives of chromotropic acid, as a large group of chromogenic reagents, have been used in the selective spectrophotometric determination of metal ions for a long period. Their chelating performance for metal ions has been studied systematically and intensively. Consequently, the accumulated information can provide basis and reference for design of newmaterials and their potential applications in phosphoproteome analysis. However, to our best knowledge, the related work has not been done. The bis-azo derivatives of chromotropic acid are typical water-soluble chromogenic reagents, which display strong retention strength toward multivalent metal ions (*i.e.* Zr^{4+}). From the literature [25], chlorophosphonazo III can react with Zr^{4+} in strongly acidic media to form stable colorful chelate with the molar extinction coefficient of 3.3×10^4. Therefore, its chromogenic analogue, *p*-hydroxychlorophosphonazo (HCPA), has been used as chelating ligand in the construction of affinity material. In addition, as the representative of mono-azo derivatives of chromotropic acid, chlorophosphonazo I (CPA I) has also been employed as ligand in IMAC material. Besides the above considerations, the good biocompatibility such as hydrophilicity of HCPA and CPA I is beneficial to efficiently and specifically isolate phosphopeptides from biological samples [17,18]. As a result, HCPA and CPA I-modified silica nanoparticles for immobilization of zirconium ions (Zr-HCPA-SNPs and Zr-CPA I-SNPs) have been designed and prepared for the selective enrichment of phosphopeptides. The purification procedures were optimized using α-casein digest, and the high efficiency and specificity of these two affinity materials in phosphopeptide enrichment were demonstrated with both the tryptic digests of standard proteins (α-casein, β-casein, ovalbumin and bovine serum albumin) and human serum.

2. Experimental

2.1. Reagents and materials

Proteins of α-casein, β-casein, ovalbumin and bovine serum albumin (BSA), and chemical reagents of 2,5-dihydroxybenzoic acid (DHB), zirconyl chloride octahydrate ($ZrOCl_2{\cdot}8H_2O$) and trifluoroacetic acid (TFA), were all obtained from Sigma (St. Louis, MO, USA). Sequencing grade modified trypsin was purchased from Promega (Madison, WI, USA). Urea, ammonium bicarbonate, 1,4-dithiothreitol, iodoacetamide and 3-glycidoxypropyltrimethoxysilane (GLYMO) were purchased from BioRad (Hercules, CA, USA). Nitric acid (HNO_3 65%, GR grade) and hydrofluoric acid (HF 40%, GR grade) were purchased from the Sinopharm Chemical Reagent Co., Ltd. (Shanghai, China). Chlorophosphonazo I (CPA I) was obtained from Chemical Factory of East China Normal University (Shanghai, China). Acetic acid (HAc) and formic acid (FA) were obtained from Aldrich (Milwaukee, WI, USA). Acetonitrile (ACN) was of chromatographic grade from Merck (Darmstadt, Germany). Deionized water used for all experiments was purified with a Milli-Q water system (Millipore, Milford, MA, USA). All other reagents and solvents were of the highest commercial quality and were used without further purification. Calibration solutions (0–10 mg L^{-1}) for P were prepared from 1000 mg L^{-1} P in 2% HNO_3 (National Institute of Metrology, China) by dilution with deionized water. Spherical silica nanoparticles with particle size of 30 nm were obtained from Wuhan Shuaier Photoelectron New Material Co., Ltd. (Wuhan, China).

2.2. Preparation of zirconium-chlorophosphonazo chelate-modified silica nanoparticles

2.2.1. Synthesis of HCPA

p-Hydroxychlorophosphonazo (HCPA) was synthesized by diazotization of 4-aminophenol and then coupling with chlorophosphonazo I (CPA I) (Fig. 1a). Briefly, 4-aminophenol was first diazotized with $NaNO_2$ in the presence of HCl at 0 °C, and then the diazotized product was coupled with CPA I by means of controlling the media pH in the range of 9–10 with a mixture of LiOH and Li_2CO_3 (molar ratio, 13.6:1) at 0–5 °C for 24 h. The resulting blue-violet colored solution was filtered, and the filtrate was acidified with 4 M HCl and placed overnight. Finally, the precipitate was washed with dilute HCl until it showed purple color, and then dried by a vacuum drier

2.2.2. Derivatization of silica nanoparticles with HCPA and CPA I

Silica nanoparticles were activated and washed with 20% HNO_3, 0.5 M NaCl, H_2O, acetone and diethyl ether, followed by desiccation at 150 °C for 4 h under vacuum for chemical modification.

The surface of activated silica nanoparticles was derivatized with 3-glycidoxypropyltrimethoxysilane (GLYMO) under absolute conditions according to a procedure by Larsson et al. [26]. The epoxy-silica was prepared as follows (Fig. 1b): 1.0 g of activated silica nanoparticles was added to a mixture of 25.0 mL of sodium dried toluene, 0.1 mL of calcium hydride dried triethylamine and 3.0 mL of GLYMO under dry nitrogen gas protection to ensure anhydrous conditions. The mixture was stirred at room temperature for 5 h and then heated to 110 °C by refluxing for 16 h. The epoxy-silica was filtered, washed with toluene, acetone and diethyl ether, and then dried at 110 °C in vacuum.

The epoxy-silica further reacted with chlorophosphonazo type derivatives of chromotropic acid (*i.e.* HCPA) using following protocol (Fig. 1c): 0.2 g of epoxy-silica and 0.5 g of HCPA were dispersed in 10 mL of absolute ethanol with addition of 0.5 mL of dry triethylamine. And then, the mixture was refluxed for 4 h to prepare HCPA-modified silica nanoparticles (HCPA-SNPs). The resulting purple colored microspheres were then filtered, washed with toluene, H_2O, 10% HAc, H_2O and MeOH, and dried at 60 °C under vacuum. The CPA I-SNPs (red) were prepared the same as the above protocol of HCPA-SNPs except the chromogenic reagent was CPA I, instead of HCPA. For electronic and steric reasons, the position of the coupling of HCPA or CPA I within the epoxy-silica, as shown in Fig. 1c, seems to be the most plausible.

2.2.3. Immobilization of zirconium ions to HCPA-SNPs and CPA I-SNPs

The zirconium-chlorophosphonazo chelate-modified silica nanoparticles were obtained by incubation of 20 mg of HCPA-SNPs or CPA I-SNPs in 20 mL of 100 mM $ZrOCl_2$ solution at room temperature overnight under gentle stirring (Fig. 1d). The obtained microspheres were centrifuged at 17,000 × *g* for 5 min. After the supernatant was removed, the microspheres were washed with water several times to remove the residue of zirconium ions. The obtained Zr-HCPA-SNPs and Zr-CPA I-SNPs were dispersed in 30% (v/v) acetonitrile (ACN) containing 0.1% (v/v) trifluoroacetic acid (TFA) solution before usage.

2.3. Digestion of HCPA-SNPs and CPA I-SNPs for phosphorus determination

The HCPA-SNPs and CPA I-SNPs were mineralized by electric heating board digestion, and the digested samples were ana-

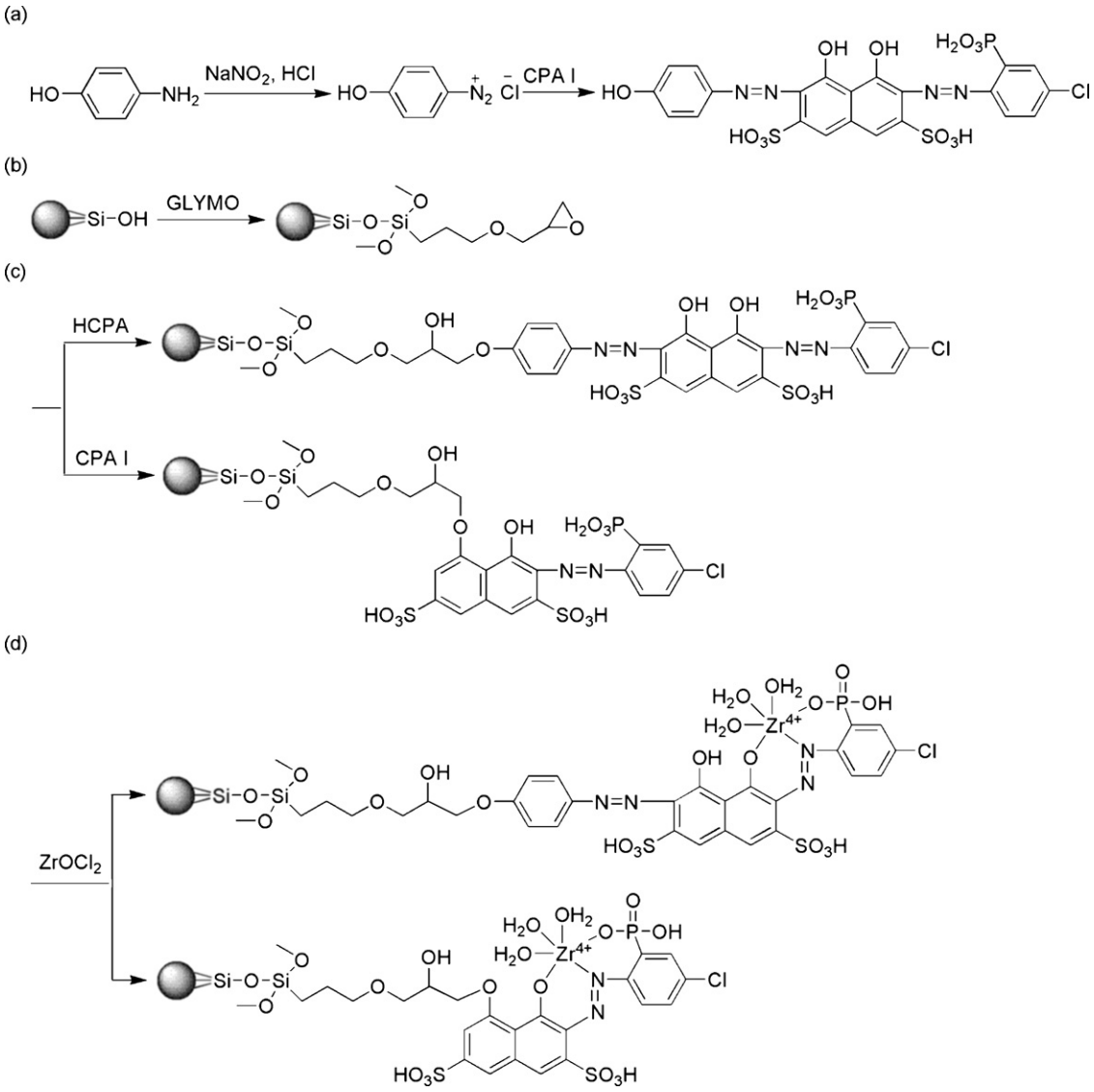

Fig. 1. Scheme for preparation of zirconium-chlorophosphonazo chelate-modified silica nanoparticles. Detailed description for each step: (a) synthesis of HCPA by diazotization of 4-aminophenol and then coupling with CPA I; (b) derivatization of a thin layer of GLYMO on the surface of silica nanoparticles; (c) coupling reaction of the epoxy-silica with HCPA and CPA I; and (d) immobilization of zirconium ions to HCPA-SNPs and CPA I-SNPs.

lyzed by inductively coupled plasma optical emission spectrometry (ICP-OES). Briefly, 50 mg of HCPA-SNPs, CPA I-SNPs and silica nanoparticles (blank) were accurately weighted into polytetrafluoroethylene vessels, and then 1.0 mL of concentrated HNO_3 and 5.0 mL of HF were added. The digestion experiments were carried out on a hot plate under watch glass covers. After cooling, 2–3 drops of concentrated HNO_3 and 2.0 mL of deionized water were added. All digestion samples were then quantitatively transferred to volumetric flask and diluted to 25 mL with water, filtered and analyzed by ICP-OES for phosphorus concentration.

2.4. Preparation of peptide samples

2.4.1. Digestion of standard proteins

Digestion of α-casein and β-casein (1 mg mL^{-1}) dissolved in 50 mM ammonium bicarbonate (pH 8.2) was carried out for 16 h at 37 °C with an enzyme-to-protein ratio of 1:50 (w/w). Ovalbumin and bovine serum albumin (BSA) (4 mg) were separately dissolved in 1.0 mL of denaturing buffer containing 8 M urea and 50 mM ammonium bicarbonate and incubated for 3 h. Then, 20 μL of 50 mM 1,4-dithiothreitol was added to the mixture and incubated at 37 °C for 2 h to reduce the disulfide bond of protein, followed by addition of 40 μL of 50 mM iodoacetamide to carbamidomethylate the resulting cysteine residues for an additional 30 min in the dark at room temperature. After that, the mixture was diluted ten times by 50 mM ammonium bicarbonate and incubated for 16 h at 37 °C with trypsin at an enzyme/substrate ratio of 1:40 (w/w) to produce proteolytic digests. All of the resulting digests were lyophilized by a vacuum concentrator and then stored in the freezer under −40 °C for further usage.

Peptide mixture 1: Peptide mixture 1 contained peptides originating from a tryptic digestion of 0.1 μM of α-casein.

Peptide mixture 2: Peptide mixture 2 contained peptides originating from tryptic digestions of 0.1 μM of each of phosphoproteins (α-casein, β-casein and ovalbumin).

Peptide mixture 3: Peptide mixture 3 contained peptides originating from tryptic digestions of phosphoproteins (α-casein, β-casein and ovalbumin) and BSA. Peptide mixture 3 with molar ratios of 1:1:1:1 and 1:1:1:10 referred to the peptide mixtures originating from tryptic digestions of 0.1 μM of each of phosphoproteins and 0.1 μM of BSA, and 0.1 μM of each of phosphoproteins and 1.0 μM of BSA, respectively.

2.4.2. Preparation of human serum samples

Human serum samples were collected from 4 healthy, 4 diabetes and 4 hypertension persons, respectively. All the samples were obtained from The Hospital of Wuhan University according to their standard clinical procedures. Briefly, blood samples were separately collected in 8.5 mL, allowed to clot at room temperature for up to 1 h, and then centrifuged at 4 °C for 5 min at 2,000 × *g*. After collection, the serum samples were aliquoted and stored at −80 °C for further usage. Before use, 10 μL of the pooled serum samples from a mixture of 4 healthy, 4 diabetes or 4 hypertension persons, respectively, were diluted with 20 μL of 2,5-dihydroxybenzoic acid (DHB) solution to a final concentration of 20 mg mL^{-1} with ACN/H_2O/TFA (50:50:0.1, v/v/v), and used directly for phosphopeptide enrichment.

2.5. Selective enrichment of phosphopeptides using Zr-HCPA-SNPs and Zr-CPA I-SNPs

Enrichment experiments were performed in "batch method" by mixing peptide samples with Zr-HCPA-SNPs or Zr-CPA I-SNPs in 0.5 mL Eppendorf microcentrifuge tubes. Peptide samples (tryptic digests of standard proteins and pooled human serum) were diluted with DHB solution, followed by addition of 5 μL of Zr-HCPA-SNPs or Zr-CPA I-SNPs (20 mg mL^{-1}). After incubation for 0.5 h under vortexing, the microspheres were separated from the supernatant by centrifugation at 17,000 × *g* for 5 min. The Zr-HCPA-SNPs or Zr-CPA I-SNPs with captured phosphopeptides were then washed with 200 μL of DHB solution and 30% ACN/0.1% TFA, respectively.

2.6. Sample preparation for MALDI-TOF MS

For on-bead analysis of phosphopeptides after enrichment, the deposition of Zr-HCPA-SNPs or Zr-CPA I-SNPs with trapped phosphopeptides was mixed with 2 μL of a matrix of 20 mg mL^{-1} DHB (in 50% ACN aqueous solution, v/v) and 1% (v/v) H_3PO_4 aqueous solution, 1:1 (v/v), and 1 μL of mixture was deposited on the plate for MALDI-TOF MS analysis.

2.7. Apparatus

The phosphorus content of HCPA-SNPs and CPA I-SNPs was determined by an inductively coupled plasma optical emission spectrometer (IRIS Intrepid II XSP, Thermo Electron, USA). MALDI-TOF MS experiments were performed in the positive reflector mode on a 4700 Proteomics Analyzer (Applied Biosystems) with the Nd:YAG laser at 355 nm, a repetition rate of 200 Hz and an acceleration voltage of 20 kV, and each mass spectrum was typically summed with 300 laser shots after being calibrated with an internal calibration using the ion signal of peptide mixtures of myoglobin.

3. Results and discussion

3.1. Design and characterization of Zr-HCPA-SNPs and Zr-CPA I-SNPs

For IMAC mode, the efficiency of phosphopeptide enrichment mainly depends on the amount of metal ions loaded with strong affinity, and the loading capacity of these metal ions is determined by the yield and stability of the formed chelates with appropriate ligands. Accordingly, the selection of suitable metal ions and chelators is of great importance in the design strategy of ideal isolation materials for phosphopeptides.

It has been well-known that zirconium (IV) displays high binding affinity for polyoxy anions (*i.e.* phosphate) due to its anion-exchange properties in acidic solution, and the high specificity and strong interaction between zirconium ions and the phosphate groups of phosphopeptides have been successfully applied to phosphopeptide enrichment [21]. Correspondingly, zirconium ions were used in our experiment. The chlorophosphonazo type derivatives of chromotropic acid, including HCPA and CPA I, with strong affinity for Zr^{4+} and good biocompatibility such as hydrophilicity, were chosen as novel ligands of affinity materials for immobilization of zirconium ions. Furthermore, GLYMO was introduced as spacer arm in the preparation of functionalized materials, which reduced the steric hindrance and facilitated the binding of phosphopeptides with immobilized Zr^{4+}. Finally, the chemical stability, high surface-to-volume ratio and ease in functionalization of silica nanoparticles make them ideal supports for derivatization. Therefore, zirconium-chlorophosphonazo chelate-modified silica nanoparticles (Zr-HCPA-SNPs and Zr-CPA I-SNPs) were prepared and applied to the selective enrichment of phosphopeptides.

Due to the same functional groups of HCPA-SNPs and CPA I-SNPs, the model of zirconium-chlorophosphonazo chelate-modified silica nanoparticles is given in Fig. 1d. For each ligand of chlorophosphonazo-functionalized beads, the hydroxyl (–OH), azo (–N=N–) and phosphate ($-PO_3H_2$) groups form the functional group for immobilization of Zr^{4+}, allowing three free sites of Zr^{4+} for phosphopeptide binding. Moreover, Zr^{4+} is chelated by two six-membered rings, avoiding the risk of metal ion leaching during the whole enrichment procedures.

The more chromogenic reagents modified on the surface of silica nanoparticles, the more zirconium ions loaded and the higher efficiency of phosphopeptide enrichment would be obtained. ICP-OES experiments were carried out to characterize the derivatized amount of P on HCPA-SNPs and CPA I-SNPs. The results show that the amount of P is 0.53 and 0.28 mg g^{-1} (corresponding to 16.94 and 8.88 μmol g^{-1}) for HCPA-SNPs and CPA I-SNPs, respectively. Taking both 100 μg of Zr-HCPA-SNPs or Zr-CPA I-SNPs and picomole level of phosphopeptides into consideration, the amount of zirconium ions loaded is 100-fold over phosphopeptides at least, which is sufficient for the selective enrichment of phosphopeptides from peptide mixtures.

3.2. Optimization of the purification procedures for Zr-HCPA-SNPs and Zr-CPA I-SNPs

For optimization of phosphopeptide enrichment, different combinations of loading and washing buffers were investigated. In the following optimization (Protocol A–C), Peptide mixture 1 (20 μL of 0.1 μM α-casein digest) was used. Protocol A: 0.01–1% FA, HAc or TFA with 50% ACN, or 10–90% ACN with 0.1% TFA, as loading buffer, 200 mM NaCl/50% ACN/0.1% TFA as washing buffer 1, and 30% ACN/0.1% TFA as washing buffer 2. Protocol B was the same as Protocol A with the exception that Peptide mixture 1 was loaded in 50% ACN/0.1% TFA. Protocol C: 20 mg mL^{-1} DHB/50% ACN/0.1% TFA as loading buffer and washing buffer 1, and 30% ACN/0.1% TFA as washing buffer 2. If not otherwise stated, Protocol C was used as the final optimized protocol for phosphopeptide enrichment by Zr-HCPA-SNPs and Zr-CPA I-SNPs in this work.

Initial optimization of the purification procedures was performed with Protocol A using Peptide mixture 1. Tryptic digest of α-casein contains abundant phosphopeptides with known phosphorylation sites and has been chosen as the typical sample to investigate the efficiency and specificity of novel enrichment methods or affinity materials. The phosphopeptides derived from α-casein and their molecular masses are shown in Table 1. The Zr-HCPA-SNPs were chosen to evaluate the efficiency and specificity of zirconium-chlorophosphonazo chelate-modified silica nanoparticles toward phosphopeptides derived from α-casein, since the functional groups of CPA I-SNPs are the same as those of HCPA-SNPs. All experiments were performed at three replicate runs to

Table 1
Detailed information of the observed phosphopeptides derived from α-casein, β-casein and ovalbumin.

Proteins	$[M+H]^+$	Phosphorylation sites	Peptide sequences
α-Casein	1466.51	1	TVDMEpSTEVFTK
	1482.60	1	TVDMEpSTEVFTK
	1539.60	2	EQLpSTpSEENSKK
	1562.04	2	EQLpSTpSEENSKK[a]
	1594.70	1	TVDMEpSTEVFTKK
	1660.79	1	VPQLEIVPNpSAEER
	1832.83	1	YLGEYLIVPNpSAEER
	1847.69	1	DIGSEpSTEDQAMEDIK
	1927.69	2	DIGpSEpSTEDQAMEDIK
	1943.70	2	DIGpSEpSTEDQAMEDIK[b]
	1951.95	1	YKVPQLEIVPNpSAEER
	2703.60	1	LRLKKYKVPQLEIVPNpSAEERL
	2720.91	5	QMEAEpSIpSpSpSEEIVPNPNpSVEQK
	2736.90	5	QMEAEpSIpSpSpSEEIVPNpSVEAQK
	3008.03	4	NANEEEYSIGpSpSpSEEpSAEVATEEVK
β-Casein	2061.83	1	FQpSEEQQQTEDELQK
	3122.27	4	RELEELNVPGEIVEpSLpSpSpSEESITR
Ovalbumin	2088.91	1	EVVGpSAEAGVDAASVSEEFR
	2511.13	1	LPGFGDpSIEAQCGTSVNVHSSLR

[a] Phosphopeptide ion peak is $[M+Na]^+$.
[b] M and pS represent oxidized methionine and phosphoserine, respectively.

get over varying signal intensities, because the ion patterns may be affected by sweet spots, diffusion process, and even the sample preparation process [27]. Evaluation of the selectivity of phosphopeptide enrichment and optimization of the enrichment conditions were carried out by comparing the number of phosphopeptides (No. (PP)) isolated from α-casein digest and the relative intensities of phosphopeptides with those of total of nonphosphopeptides (I (PP)/I (NPP)) in the same spectrum.

3.2.1. Influence of acids and their concentrations in loading buffer for binding properties of Zr-HCPA-SNPs

The pH effect is the most important factor that controls the efficiency and specificity of phosphopeptide enrichment. In our experiments, three different acids (FA, HAc and TFA) at various concentrations (0.01–1%) in loading buffer were used to investigate the effect of pH control on the selective binding of phosphopeptides to Zr-HCPA-SNPs. Fig. 2 shows a strong pH-dependency of binding properties. As indicated in Fig. 2, 0.1% TFA gave the best performance of phosphopeptide enrichment for Zr-HCPA-SNPs. Low concentrations of acids resulted in poor selectivity of phosphopeptide enrichment due to the competitive binding and ion suppression from nonphosphopeptides, whereas higher concentrations protonated the carboxyl groups of nonphosphopeptides as well as partial phosphate groups of phosphopeptides, which are both ineffective for phosphopeptide enrichment by Zr-HCPA-SNPs. As for FA used in phosphopeptide enrichment, both No. (PP) and I (PP)/I (NPP) were enhanced with the increase of FA concentration (Fig. 2). However, further raising FA concentration led to poor enrichment of phosphopeptides (data not shown). On the basis of the above analysis, it can be seen that the efficiency and specificity of phosphopeptide enrichment from α-casein digest by Zr-HCPA-SNPs increase in the following order: TFA > FA > HAc. Acids used in buffer system not only provide appropriate pH values to discriminate dissociated phosphates of phosphopeptides from neutral

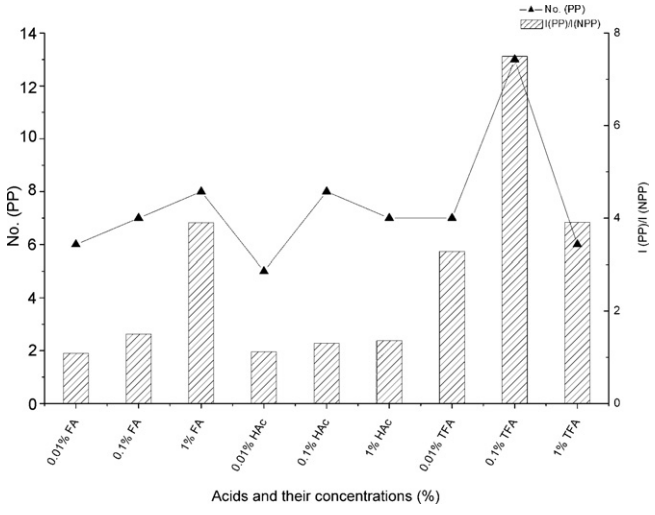

Fig. 2. Effect of acids and their concentrations on the selective enrichment of phosphopeptides by Zr-HCPA-SNPs. Peptide mixture 1 (20 μL of 0.1 μM α-casein digest) was enriched using different acids (FA, HAc and TFA) at various concentrations (0.01–1%) in loading buffer. The line graph (▲) together with left *y*-axis shows the number of phosphopeptides (No. (PP)) isolated from α-casein digest, and the bar graph together with right *y*-axis shows the peak intensities of phosphopeptides dividing those of total nonphosphopeptides (I (PP)/I (NPP)) in the same spectrum. Three spot replicates were taken in the experiments and were used to calculate the average ion count. PP = Phosphopeptides, NPP = Nonphosphopeptides.

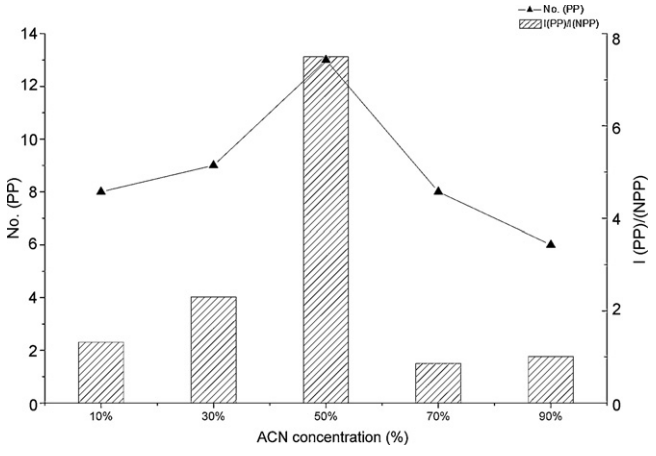

Fig. 3. Effect of ACN concentration on the selective enrichment of phosphopeptides by Zr-HCPA-SNPs. Peptide mixture 1 (20 μL of 0.1 μM α-casein digest) was enriched using different acetonitrile concentrations (10–90%) in loading buffer. The line graph (▲) together with left *y*-axis shows the number of phosphopeptides (No. (PP)) isolated from α-casein digest, and the bar graph together with right *y*-axis shows the peak intensities of phosphopeptides dividing those of total nonphosphopeptides (I (PP)/I (NPP)) in the same spectrum. Three spot replicates were taken in the experiments and were used to calculate the average ion count. PP = Phosphopeptides, NPP = Nonphosphopeptides.

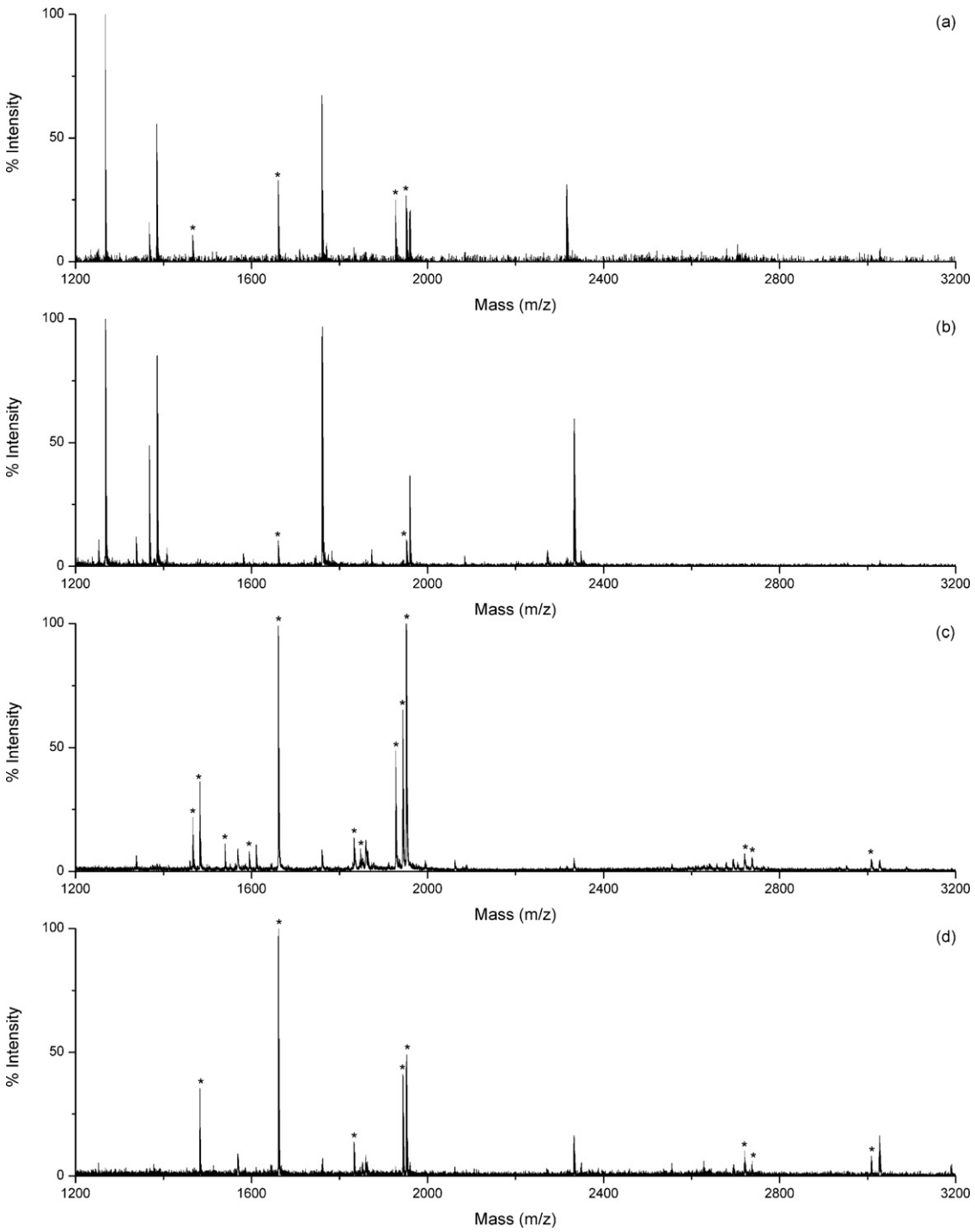

Fig. 4. MALDI mass spectra of the tryptic digest of α-casein (2 pmol). (a) Direct analysis; (b) analysis of the residual solution after phosphopeptide enrichment by Zr-HCPA-SNPs; on-bead analysis of phosphopeptides enriched from Peptide mixture 1 (20 μL of 0.1 μM α-casein digest) with Protocol B (50% ACN/0.1% TFA as the initial optimized buffer) by (c) Zr-HCPA-SNPs, and (d) Zr-CPA I-SNPs. The phosphopeptides derived from α-casein are marked with *.

carboxyl groups of nonphosphopeptides, but also act as additives with the structures of containing carboxylic acid groups to inhibit nonspecific binding of acidic residues to metal ions. Although the structures of FA, HAc and TFA contain one common carboxylic acid group, different alkyl groups with the structures of electron withdrawal or steric hindrance to compete with nonphosphopeptide binding determine different efficiency and specificity of phosphopeptide enrichment [19].

Therefore, the use of 0.1% TFA with optimal pH value in loading buffer was suitable for the selective enrichment of phosphopeptides, which protonated carboxyl groups but still dissociated phosphate groups, allowing the discrimination of phosphoamino acids from acidic residues on Zr-HCPA-SNPs.

3.2.2. Influence of ACN and its concentration in loading buffer for binding properties of Zr-HCPA-SNPs

The effect of ACN at different concentrations (10–90%) on phosphopeptide enrichment with Zr-HCPA-SNPs is also investigated. An appropriate concentration of ACN not only prevented weak hydrophobic interaction between nonphosphopeptides and Zr-

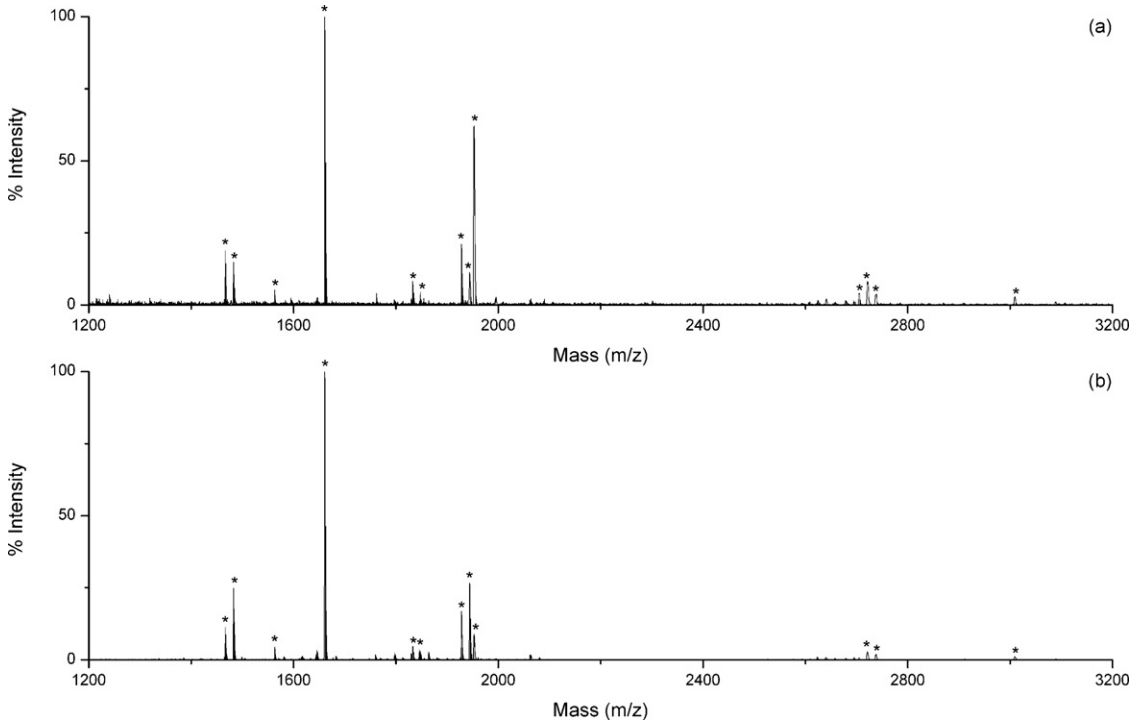

Fig. 5. Effect of the addition of DHB to loading and washing buffers on the selective enrichment of phosphopeptides from Peptide mixture 1 (20 μL of 0.1 μM α-casein digest) with Protocol C (20 mg mL^{-1} DHB/50% ACN/0.1% TFA as the final optimized buffer) by (a) Zr-HCPA-SNPs, and (b) Zr-CPA I-SNPs. The phosphopeptides derived from α-casein are marked with *.

HCPA-SNPs, but also enhanced binding between phosphate groups and immobilized metal ions. It can be found from Fig. 3 that the use of 50% ACN in buffer system is the best. Low concentration of ACN in loading buffer did not effectively decrease the hydrophobic interaction, whereas higher concentration was not beneficial for the dissociation of the phosphate groups of phosphopeptides in aqueous solution and their coordination with immobilized zirconium ions. Therefore, 50% ACN/0.1% TFA (Protocol B) as the initial optimized buffer for phosphopeptide enrichment was used in the following experiments.

3.2.3. *MALDI mass spectra of the initial optimized conditions*

For direct analysis, tryptic digest of 2 pmol of commercial α-casein was carried out by MALDI-TOF MS. As shown in Fig. 4a, only 4 phosphopeptide peaks appeared in the spectrum and the peaks of phosphopeptides were difficult to be distinguished from the numerous nonphosphopeptides. Furthermore, most of the phosphopeptides containing multiple phosphorylation sites were hard to detect by direct MALDI-TOF MS analysis due to low ionization efficiency and serious suppression of nonphosphopeptides. However, the number of phosphopeptides was significantly increased and the intensities were obviously improved when Zr-HCPA-SNPs and Zr-CPA I-SNPs were applied to isolate phosphopeptides from Peptide mixture 1 (20 μL of 0.1 μM α-casein digest) with Protocol B (50% ACN/0.1% TFA as the initial optimized buffer) prior to MALDI-TOF MS analysis (Fig. 4c and d). As many as 13 and 8 phosphopeptides were detected for Zr-HCPA-SNPs and Zr-CPA I-SNPs, respectively, and the phosphopeptide peaks at *m/z* 1660.79 and 1951.95 constituted the most abundant peaks dominating the mass spectra. After phosphopeptide enrichment by Zr-HCPA-SNPs and Zr-CPA I-SNPs, the highly abundant peaks of nonphosphopeptides from α-casein digest were effectively eliminated and only few nonphosphopeptide peaks with very low intensities still appeared in the spectra. In addition, the residual solution after phosphopeptide enrichment by Zr-HCPA-SNPs from 2 pmol α-casein digest was also analyzed by MALDI-TOF MS (Fig. 4b). Only two weak phosphopeptide peaks at *m/z* 1660.79 and 1951.95 could be observed. These facts demonstrate that Zr-HCPA-SNPs and Zr-CPA I-SNPs can effectively isolate phosphopeptides from proteolytic digests. On the basis of these initial studies, the conditions of phosphopeptide enrichment with Zr-HCPA-SNPs and Zr-CPA I-SNPs have been optimized in detail further.

3.2.4. *Effect of DHB in loading and washing buffers on the selective enrichment of phosphopeptides for Zr-HCPA-SNPs and Zr-CPA I-SNPs*

In addition to inorganic acids, organic solvents and salts, additives have been included in loading and washing buffers to improve the selectivity of phosphopeptide enrichment. It has been reported that additives such as DHB in buffer system can reduce nonspecific binding of nonphosphopeptides while retain the high binding affinity for phosphopeptides [22]. Thus, the possibility of adding DHB to loading and washing buffers in the improvement of the selectivity was also investigated. Peptide mixture 1 (20 μL of 0.1 μM α-casein digest) was loaded onto Zr-HCPA-SNPs and Zr-CPA I-SNPs in DHB solution (20 mg mL^{-1} DHB/50% ACN/0.1% TFA), and the microspheres were subsequently washed with 200 μL of DHB solution and 30% ACN/0.1%TFA, respectively (Protocol C). After the addition of DHB in buffer system, 13 and 12 phosphopeptides were detected for Zr-HCPA-SNPs and Zr-CPA I-SNPs, respectively, and the selectivity of phosphopeptide enrichment was dramatically enhanced for these two affinity materials in the mass spectra (Fig. 5). Furthermore, the number of phosphopeptides isolated from α-casein digest was slightly increased for Zr-CPA I-SNPs (Fig. 5b) compared with the protocol without DHB in loading and washing buffers (Fig. 4d). Our experiments indicate that the addition of DHB (20 mg mL^{-1}) to loading and washing buffers is sufficient to displace the bound acidic residues by competitive binding of DHB with immobilized zirconium ions on the surface of silica nanoparticles thereby increasing the selective binding of phosphopeptides. Con-

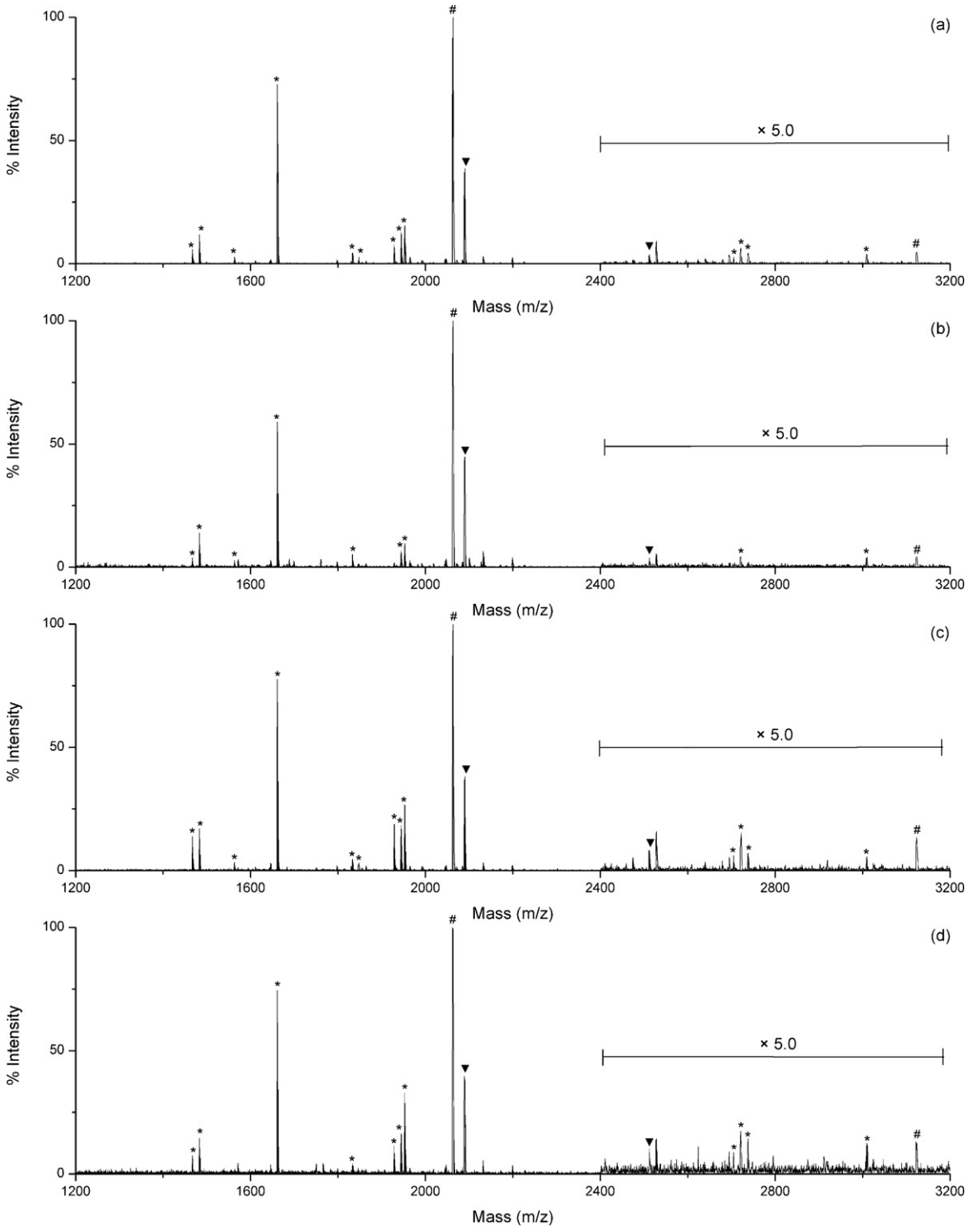

Fig. 6. Enrichment of phosphopeptides from peptide mixtures (20 μL of tryptic digests of α-casein, β-casein, ovalbumin and BSA with different molar ratios) by different zirconium-chlorophosphonazo chelate-modified silica nanoparticles: (a) Zr-HCPA-SNPs (ratio 1:1:1:0, Peptide mixture 2), (b) Zr-CPA I-SNPs (ratio 1:1:1:0, Peptide mixture 2), (c) Zr-HCPA-SNPs (ratio 1:1:1:1, Peptide mixture 3), and (d) Zr-HCPA-SNPs (ratio 1:1:1:10, Peptide mixture 3). The phosphopeptides derived from α-casein, β-casein and ovalbumin are marked with *, # and ▼, respectively.

siderable effort by increasing DHB concentration to 300 mg mL^{-1} did not completely abrogate the adsorption of nonphosphopeptides to Zr-HCPA-SNPs and Zr-CPA I-SNPs. On the contrary, high concentration of DHB (300 mg mL^{-1}) exhibited poorer performance of phosphopeptide enrichment than that of 20 mg mL^{-1} DHB (data not shown), which suggests large molar excess of DHB molecules effectively compete with both nonphosphopeptides and phosphopeptides for biding sites on the surface of Zr-HCPA-SNPs and Zr-CPA I-SNPs, leading to weak signal-to-noise (S/N) of phosphopeptide peaks in the mass spectra. As a result, Protocol C (20 mg mL^{-1} DHB/50% ACN/0.1% TFA) was chosen as the final optimized buffer for the following experiments.

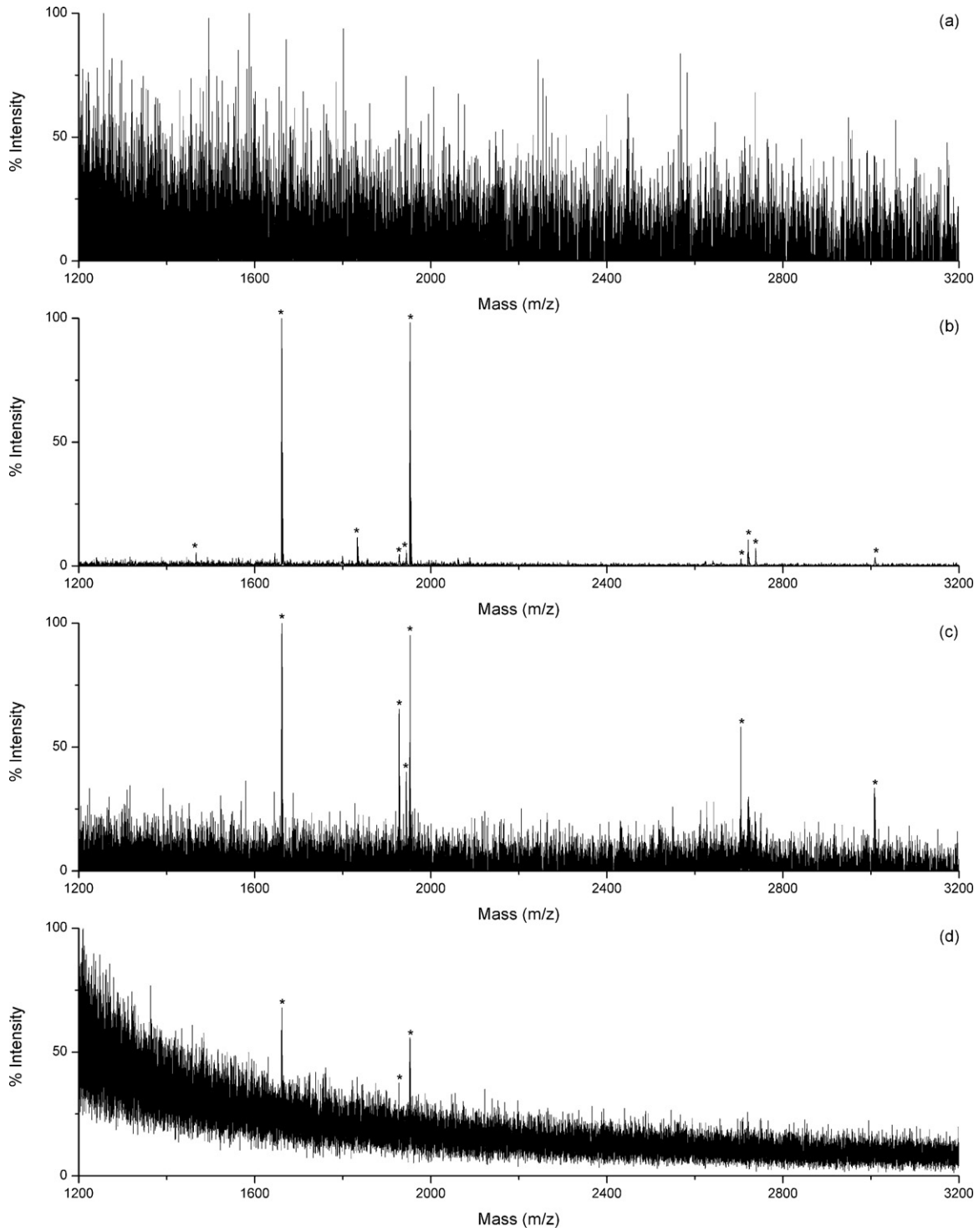

Fig. 7. MALDI mass spectra of α-casein digest. (a) Control experiment of Peptide mixture 1 (20 μL of 0.1 μM α-casein digest) isolated by HCPA-SNPs; tryptic digest of α-casein (10 μL) following enrichment of Zr-HCPA-SNPs with different concentrations: (b) 0.1 μM, (c) 0.01 μM, and (d) 0.005 μM. The phosphopeptides derived from α-casein are marked with *.

3.3. Enrichment of phosphopeptides from complex peptide mixtures using Zr-HCPA-SNPs and Zr-CPA I-SNPs

In order to evaluate the feasibility of Zr-HCPA-SNPs and Zr-CPA I-SNPs to capture phosphopeptides from complex peptide samples, tryptic digests of three standard phosphoproteins, α-casein, β-casein and ovalbumin, with a molar ratio of 1:1:1 (Peptide mixture 2, 20 μL) were used. As shown in Fig. 6a and b, the number of phosphopeptides enriched from the tryptic digests of phosphoproteins and specificity of phosphopeptide enrichment were comprehensively compared with these two affinity materials. The results indicate that Zr-HCPA-SNPs (capture of 13 phosphopeptides derived from α-casein, 2 from β-casein and 2 from ovalbumin, 13α2β2O) are better than Zr-CPA I-SNPs (9α2β2O) for efficient and specific enrichment of phosphopeptides. The differences of Zr-HCPA-SNPs and Zr-CPA I-SNPs for the selective enrichment of phosphopeptides mainly resulted from the derivatized amount of HCPA and CPA I on the surface of silica nanoparticles in the presence

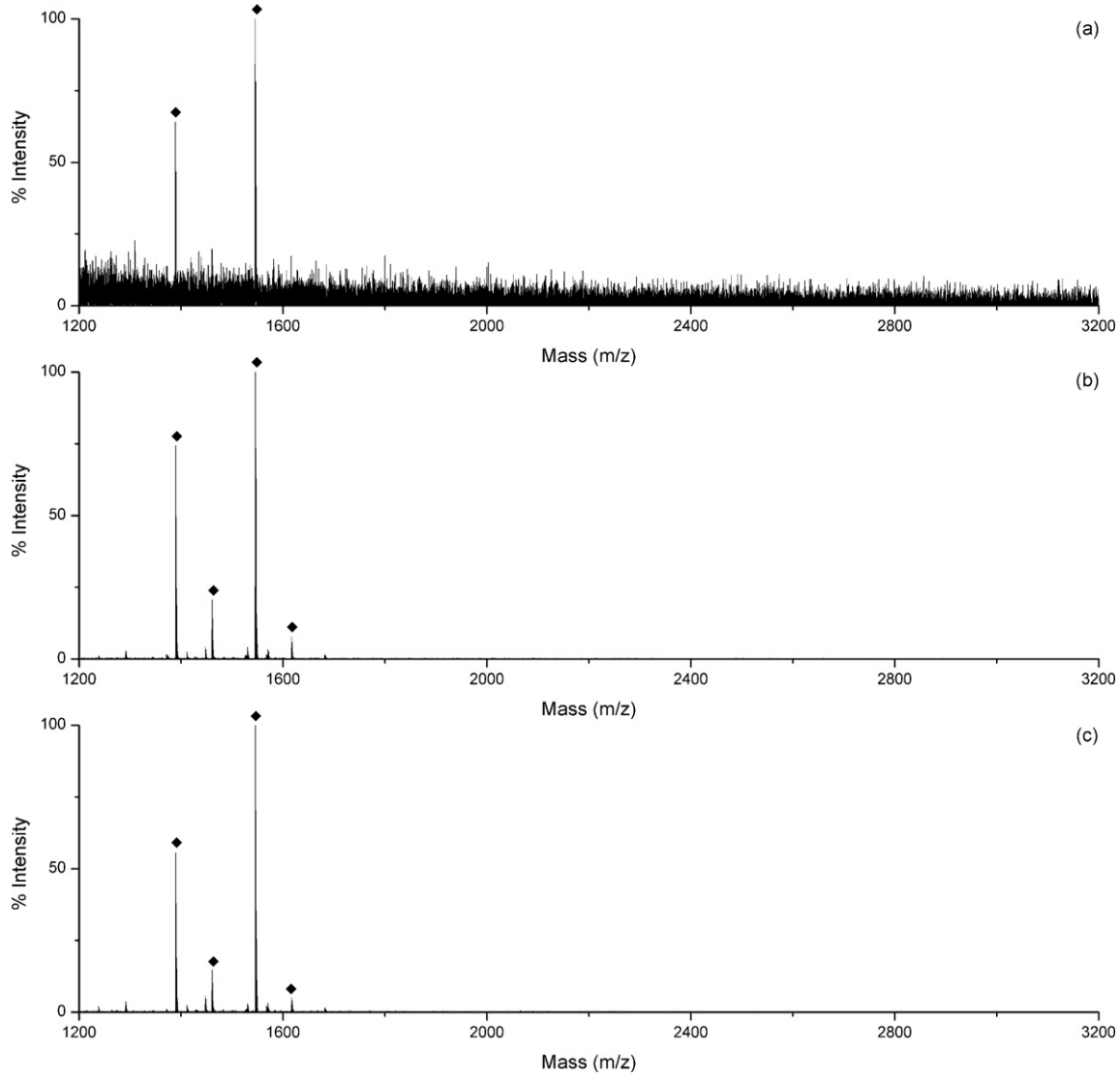

Fig. 8. MALDI mass spectra of phosphopeptides enriched by Zr-HCPA-SNPs from pooled human serum of (a) healthy, (b) diabetes, and (c) hypertension persons. The phosphopeptides derived from fibrinogen protein are marked with ♦.

of excess chromogenic reagents. One of the possible reasons for the low amount of chelating ligands on CPA I-SNPs is that the naphthalic hydroxyl group of CPA I with big steric hindrance obstructs the access of epoxy group on the surface of epoxy-silica.

The Zr-HCPA-SNPs with better performance of phosphopeptide enrichment were selected to isolate phosphopeptides from more complex peptide mixtures. Peptide mixture 3 (20 μL of tryptic digests of α-casein, β-casein, ovalbumin and BSA, with molar ratios of 1:1:1:1 and 1:1:1:10, respectively) was used to further test the efficiency and specificity of phosphopeptide enrichment using Zr-HCPA-SNPs. In total 17 phosphopeptides were isolated by Zr-HCPA-SNPs (13α2β2O) when Peptide mixture 3 (ratio, 1:1:1:1) was loaded (Fig. 6c). The results of Zr-HCPA-SNPs for the selective enrichment of phosphopeptides from Peptide mixture 3 (ratio, 1:1:1:1) were similar to those of Peptide mixture 2 (Fig. 6a), indicating that the inclusion of the tryptic digest of BSA with the same amount as phosphoprotein in peptide mixture did not dramatically decline the efficiency and specificity of phosphopeptide enrichment. Furthermore, Zr-HCPA-SNPs (11α2β2O) displayed excellent performance in the isolation of phosphopeptides when the molar ratio of the tryptic digests of phosphoproteins to nonphosphoprotein (BSA) was decreased to 1:10 (Fig. 6d), which is close to the stoichiometric population of phosphoproteins in real biological samples.

3.4. Control experiment and detection limit

To investigate nonspecific interaction of peptides on the raw functionalized silica nanoparticles, a control experiment was performed by HCPA-SNPs using the same optimized enrichment conditions as those used for Zr-HCPA-SNPs. No phosphopeptide peaks were observed in the spectrum (Fig. 7a) compared with those in Fig. 5a, which indicates that there is no obvious nonspecific binding of peptides on HCPA-modified silica nanoparticles. Therefore, the specific capture of phosphopeptides by Zr-HCPA-SNPs mainly resulted from the strong interaction of phosphopeptides with zirconium ions immobilized on the surface of silica nanoparticles.

The sensitivity of phosphopeptide enrichment using Zr-HCPA-SNPs was determined from the tryptic digest of α-casein under the optimized enrichment conditions. The Zr-HCPA-SNPs were used to isolate phosphopeptides from α-casein digest present in low concentration (0.1, 0.01, and 0.005 μM, respectively) with fixed volume (10 μL). Fig. 7b–d shows the MALDI-TOF mass spectra of the

Table 2
Phosphorylated fragments degraded from fibrinogen protein in human serum..

Protein	$[M+H]^+$	Phosphorylation sites	Peptide sequences
Fibrinogen	1389.31	1	DpSGEGDFLAEGGGV
	1460.39	1	ADpSGEGDFLAEGGGV
	1545.50	1	DpSGEGDFLAEGGGVR
	1616.57	1	ADpSGEGDFLAEGGGVR

pS represents phosphoserine.

trapped phosphopeptides by Zr-HCPA-SNPs from α-casein digest with amount of 1000, 100, and 50 fmol, in which 10, 6, and 3 phosphopeptides were detected, respectively. If the minimum of three phosphopeptides is defined as the detection limit, the detection limit with Zr-HCPA-SNPs enrichment from α-casein digest by MALDI-TOF MS analysis is close to 50 fmol, revealing the high efficiency and specificity of Zr-HCPA-SNPs for phosphoproteome analysis.

3.5. Enrichment of phosphopeptides from pooled human serum using Zr-HCPA-SNPs

Phosphopeptides are present in low abundance in human serum but play an important role in regulatory mechanisms and may serve as a casual factor in diseases. The enrichment and analysis of phosphopeptides directly from human serum is a large challenge for researchers involved in phosphoproteomics. Hence, the applicability of Zr-HCPA-SNPs microspheres in direct and selective enrichment of phosphopeptides in human serum has also been investigated. Before enrichment, the human serum was just diluted and without any other pretreatment. Fig. 8 displays the results. As many as 2, 4 and 4 phosphopeptides were detected in the serum of healthy, diabetes and hypertension persons, respectively. The peptide sequences and phosphorylation sites of the phosphopeptide residues (*m/z* at 1389.31, 1460.39, 1545.50 and 1616.57) have been identified before [28,29]. The four phosphopeptide residues are all matched to residues derived from fibrinopeptide A (gi|229185, ADSGEGDFLAEGGGVR) whose increased level can be found in hepatocellular, ovarian, urothelial, and gastric cancers [30–33]. Detailed information of the phosphorylated fragments degraded from fibrinogen protein is listed in Table 2. It can be clearly seen that the phosphopeptides in human serum express differently among healthy, diabetes and hypertension persons. The two phosphopeptide peaks at *m/z* 1460.39, and 1616.57 appeared in Fig. 8b and c may be the degraded fragments from fibrinopeptide A by proteases compared with those in Fig. 8a. Our results reveal that different diseases may cause the differences in the expression levels of phosphorylated fibrinogen fragments in human serum.

4. Conclusions

Two novel adsorbents with chlorophosphonazo type derivatives of chromotropic acid (HCPA and CPA I) as chelating ligands, zirconium ions as immobilized metal ions, GLYMO as spacer arm and silica nanoparticles as supports, were prepared and applied to the selective enrichment of phosphopeptides. The enrichment conditions (acids, ACN and DHB) for zirconium-chlorophosphonazo chelate-modified silica nanoparticles were optimized using α-casein digest. Our experiments show that the best results are achieved with a loading/washing buffer solution of 20 mg mL^{-1} DHB in 0.1% TFA in 50:50 ACN–H_2O. With the optimized buffer system, the efficiency and specificity of Zr-HCPA-SNPs and Zr-CPA I-SNPs for phosphopeptides were demonstrated with the tryptic digests of standard proteins (α-casein, β-casein, ovalbumin and BSA). The performance of Zr-HCPA-SNPs in phosphopeptide enrichment is better than that of Zr-CPA I-SNPs, mainly because the derivatized amount of HCPA on the surface of silica nanoparticles is larger than that of CPA I. The detection limit by MALDI-TOF MS analysis with Zr-HCPA-SNPs enrichment from α-casein digest was close to 50 fmol. The strong and specific affinity between zirconium ions and phosphopeptides, the good biocompatibility such as hydrophilicity of ligands, the presence of spacer arm, and the high surface-to-volume ratio of nanoparticles contribute to the high performance of Zr-HCPA-SNPs in phosphopeptide enrichment. Finally, the feasibility of Zr-HCPA-SNPs in real samples was demonstrated in direct enrichment of phosphopeptides in diluted human serum for MALDI-TOF MS analysis. The results indicate that the phosphopeptide expressions are remarkably different among healthy, diabetes and hypertension individuals. This work is expected to exploit new applications of chromogenic reagents in the preparation of novel IMAC materials and hopeful potentials in disease diagnosis, biomarker screening and elucidation of the pathogenesis process of diseases.

Acknowledgements

This work was supported by the National Natural Science Foundation of China (20775058, 20835004 and 30770550), the Special Research Fund for the Doctoral Program of Higher Education of China (20070486031) and the Fundamental Research Funds for the Central Universities (1101004).

References

[1] J.D. Graves, E.G. Krebs, Pharmacol. Ther. 82 (1999) 111.
[2] T. Hunter, Cell 100 (2000) 113.
[3] M. Bollen, M. Beullens, Trends Cell Biol. 12 (2002) 138.
[4] S. Zolnierowicz, M. Bollen, EMBO J. 19 (2000) 483.
[5] D.T. McLachlin, B.T. Chait, Curr. Opin. Chem. Biol. 5 (2001) 591.
[6] M. Mann, S.E. Ong, M. Gronborg, H. Steen, O.N. Jensen, A. Pandey, Trends Biotechnol. 20 (2002) 261.
[7] R.E. Schweppe, C.E. Haydon, T.A. Lewis, K.A. Resing, N.G. Ahn, Acc. Chem. Res. 36 (2003) 453.
[8] T.T. Yip, T.W. Hutchens, FEBS Lett. 308 (1992) 149.
[9] R.S. Annan, S.A. Carr, Anal. Chem. 68 (1996) 3413.
[10] K.L. Bennett, A. Stensballe, A.V. Podtelejnikov, M. Moniatte, O.N. Jensen, J. Mass Spectrom. 37 (2002) 179.
[11] M.W.H. Pinkse, P.M. Uitto, M.J. Hilhorst, B. Ooms, A.J.R. Heck, Anal. Chem. 76 (2004) 3935.
[12] J.L. Wang, Y.J. Zhang, H. Jiang, Y. Cai, X.H. Qian, Proteomics 6 (2006) 404.
[13] J. Rush, A. Moritz, K.A. Lee, A. Guo, V.L. Goss, E.J. Spek, H. Zhang, X.M. Zha, R.D. Polakiewicz, M.J. Comb, Nat. Biotechnol. 23 (2005) 94.
[14] A.M. Hinsby, J.V. Olsen, M. Mann, J. Biol. Chem. 279 (2004) 46438.
[15] H. Zhou, J.D. Watts, R. Aebersold, Nat. Biotechnol. 19 (2001) 375.
[16] D.T. McLachlin, B.T. Chait, Anal. Chem. 75 (2003) 6826.
[17] S. Feng, M.L. Ye, H.J. Zhou, X.G. Jiang, X.N. Jiang, H.F. Zou, B.L. Gong, Mol. Cell. Proteomics 6 (2007) 1656.
[18] H.J. Zhou, M.L. Ye, J. Dong, G.H. Han, X.N. Jiang, R.N. Wu, H.F. Zou, J. Proteome Res. 7 (2008) 3957.
[19] C.F. Tsai, Y.T. Wang, Y.R. Chen, C.Y. Lai, P.Y. Lin, K.T. Pan, J.Y. Chen, K.H. Khoo, Y.J. Chen, J. Proteome Res. 7 (2008) 4058.
[20] M.C. Posewitz, P. Tempst, Anal. Chem. 71 (1999) 2883.
[21] H.K. Kweon, K. Hakansson, Anal. Chem. 78 (2006) 1743.
[22] M.R. Larsen, T.E. Thingholm, O.N. Jensen, P. Roepstorff, T.J.D. Jorgensen, Mol. Cell. Proteomics 4 (2005) 873.
[23] B.A. Ballif, J. Villen, S.A. Beausoleil, D. Schwartz, S.P. Gygi, Mol. Cell. Proteomics 3 (2004) 1093.
[24] T.S. Nuhse, A. Stensballe, O.N. Jensen, S.C. Peck, Mol. Cell. Proteomics 2 (2003) 1234.
[25] V.I. Fadeeva, I.P. Alimarin, Zhur. Anal. Khim. 17 (1962) 1020.
[26] P.O. Larsson, M. Glad, L. Hansson, M.O. Mansson, S. Ohlson, K. Mosbach, Adv. Chromatogr. 21 (1983) 41.
[27] L. Trojer, G. Stecher, I. Feuerstein, G.K. Bonn, Rapid Commun. Mass Spectrom. 19 (2005) 3398.
[28] Y. Li, D.W. Qi, C.H. Deng, P.Y. Yang, X.M. Zhang, J. Proteome Res. 7 (2008) 1767.

[29] L.H. Hu, H.J. Zhou, Y.H. Li, S.T. Sun, L.H. Guo, M.L. Ye, X.F. Tian, J.R. Gu, S.L. Yang, H.F. Zou, Anal. Chem. 81 (2009) 94.
[30] D. Theodorescu, S. Wittke, M.M. Ross, M. Walden, M. Conaway, I. Just, H. Mischak, H.F. Frierson, Lancet Oncol. 7 (2006) 230.
[31] H.R. Bergen, G. Vasmatzis, W.A. Cliby, K.L. Johnson, A.L. Oberg, D.C. Muddiman, Dis. Markers 19 (2003) 239.
[32] E. Orvisky, S.K. Drake, B.M. Martin, M. Abdel-Hamid, H.W. Ressom, R.S. Varghese, Y. An, D. Saha, G.L. Hortin, C.A. Loffredo, R. Goldman, Proteomics 6 (2006) 2895.
[33] M.P.A. Ebert, D. Niemeyer, S.O. Deininger, T. Wex, C. Knippig, J. Hoffmann, J. Sauer, W. Albrecht, P. Malfertheiner, C. Rocken, J. Proteome Res. 5 (2006) 2152.